On the use of Cu:Be clamp cells in magnetization and neutron scattering studies

2005 J. Phys.: Condens. Matter 17 S3111

(http://iopscience.iop.org/0953-8984/17/40/014)

INSTITUTE OF PHYSICS PUBLISHING JOURNAL OF PHYSICS: CONDENSED MATTER

J. Phys.: Condens. Matter **17** (2005) S3111–S3120 doi:10.1088/0953-8984/17/40/014

On the use of Cu:Be clamp cells in magnetization and neutron scattering studies

C Pfleiderer[1,4], **A D Huxley**[2] **and S M Hayden**[3]

[1] Physikalisches Institut, Universität Karlsruhe, D-76128 Karlsruhe, Germany
[2] DRFMC-SPSMS, CEA Grenoble, F-38054 Grenoble Cedex 9, France
[3] HH Wills Physics Laboratory, University of Bristol, Bristol BS8 1TL, UK

Received 8 July 2005
Published 23 September 2005
Online at stacks.iop.org/JPhysCM/17/S3111

Abstract

The use of miniature clamp cells made of Cu:Be for magnetization and neutron scattering studies in the medium pressure range is reviewed by giving recent results achieved in studies of UGe_2, MnSi and $ZrZn_2$. The experiments reviewed here establish in particular that small samples can be studied rather well at high pressures using a variety of different techniques, notably conventional diffraction, cold and thermal neutron triple axes and small-angle neutron scattering.

(Some figures in this article are in colour only in the electronic version)

1. Scientific challenges in the medium pressure range

In the past decade hydrostatic pressure has become a widely used experimental tool in the study of d- and f-electron materials. The appeal of hydrostatic pressure as compared to compositional tuning lies in the possibility of changing the material properties without introducing additional complexities related to defects. In the so-called 'medium pressure range' (10–30 kbar) a number of discoveries have generated great scientific interest. For instance, when long-range antiferromagnetism is forced to vanish in the itinerant-electron systems $CePd_2Si_2$ and $CeIn_3$ [1] at pressures of 28 and 25 kbar, respectively, superconductivity emerges in a small dome that appears to mask the point where $T_N \to 0$. In the itinerant ferromagnet UGe_2, on the other hand, a superconducting dome has been discovered [2, 3] that appears to be centred on the first-order boundary between two ferromagnetic phases [4]. In the d-electron system MnSi evidence for an extended non-Fermi liquid (NFL) phase has been found above $p_c = 14.6$ kbar [5–7], where the discovery of partial magnetic order in a phase pocket within the NFL phase has attracted additional interest [8]. The observation of a first-order suppression of ferromagnetism at $p_c = 16.5$ kbar in the C15 Laves phase $ZrZn_2$ [9] has, finally, led to the speculation that ferromagnetic quantum critical points may not exist in general.

[4] Author to whom any correspondence should be addressed. Present address: Physik Department E21, Technische Universität München, D-85748 Garching, Germany.

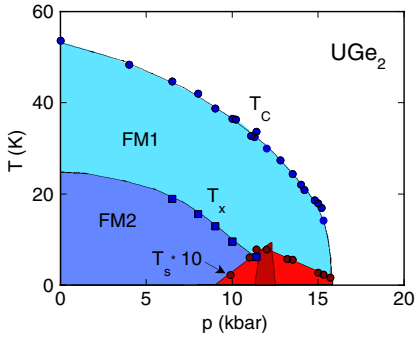

Figure 1. Temperature versus pressure phase diagram of UGe_2 at ambient magnetic field. See text and references [2–4] for details.

The initial discovery of these phenomena was based on measurements of the resistivity and AC susceptibility. For a deep understanding of the underlying physics, however, measurements of the DC magnetization and neutron scattering have become essential. This normally requires nonmagnetic pressure cells for the study of large sample volumes. Neutron scattering under pressure is more difficult, since the pressure cell both restricts the solid angle over which data can be collected and significantly absorbs the incident and diffracted beams. On the other hand, samples of sufficient quality to observe the phenomena of interest tend to be small, so the pressure apparatus used for these studies does not need to be large.

In principle, two types of techniques may be used to generate high pressures for the study of intermetallic compounds: first, clamp-type pressure cells at low and medium pressures and, second, anvil-type pressure cells at medium and high pressures. Even though these two techniques overlap in the medium pressure range, studies in this regime tend to be extremely difficult. Clamp-type pressure cells, which offer the advantage of large sample volumes, tend to be unreliable above 10 kbar due to the limitations of the strength of the cell material. Anvil-type pressure cells, on the other hand, have the disadvantage of very small sample volumes and the sealing tends to be unreliable at the lower pressure boundary.

In this paper we review recent work using nonmagnetic miniature clamp-type pressure cells made of Cu:Be. The pressure cells are in every respect identical to conventional clamp cells [10, 11], however, with a reduced overall size. The outer diameter is typically 12 mm, with a 3 mm bore that permits the study of samples with a diameter of up to 2.5 mm. To achieve the highest pressures the Cu:Be cell was carefully autofrettaged. For sealing, PTFE capsules are used and the pressure transmitter is Fluorinert. The review presented here aims to advertize that nonmagnetic miniature clamp cells made of Cu:Be can be extremely useful in magnetization as well as various neutron scattering techniques by providing prominent examples.

2. The ferromagnetism of UGe_2 at high pressure

In UGe_2, itinerant-electron ferromagnetism sets in below a Curie temperature $T_C = 52$ K, where the ferromagnetic state at ambient pressure is strongly uniaxial. With increasing pressure T_C decreases monotonically and vanishes continuously at $p_c = 16$ kbar. The emergence of a superconducting dome in the ferromagnetic state of UGe_2 [2, 3], centred at the border of two ferromagnetic phases at $p_x = 12.5$ kbar, has created great scientific interest (figure 1). Key questions concern (i) the nature and interplay of the ferromagnetic phases above and below p_x, and (ii) the microscopic coexistence of the ferromagnetism and superconductivity. These may be addressed in neutron scattering and magnetization studies at high pressure. Detailed reports of the work reviewed here have been given in [12, 13].

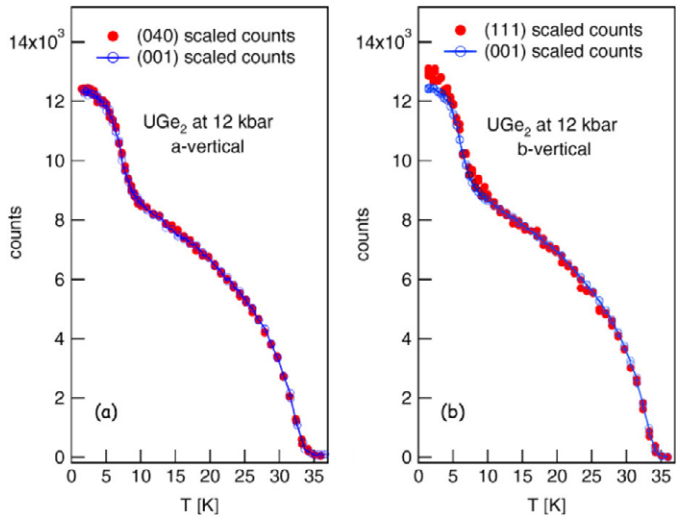

Figure 2. Temperature dependence of the different nuclear Bragg peaks in UGe_2 at a pressure of 12 kbar. (a) Qualitative comparison of the scaled (040) and (001) Bragg intensities. (b) Comparison of the scaled (111) with (001) Bragg intensities. See [12] for further details.

In the experiments addressed in the following, the use of small high-quality single crystals in combination with the nonmagnetic Cu:Be clamp cell described above proved to be advantageous in two ways. First, precise adjustment of the pressure prior to the experiments allowed efficient use of the neutron beam time. Second, direct comparison of the uniform magnetization measured in a vibrating sample magnetometer (VSM) with the microscopic magnetic polarization as measured by neutron diffraction provided information about the nature of the ferromagnetic state. Experiments were carried out at the D23-CRG instrument at the Institute Laue Langevin (ILL), where neutrons at a wavelength of 2.37 Å were used. Two samples oriented with the (100) and (010) axes perpendicular to the diffraction plane were mounted in the same pressure cell and measured one after the other without warming the clamp cell.

A complete polarized neutron diffraction study of UGe_2 at ambient pressure was reported by Kernavanois *et al* [14]. It was found that the measured moment distribution may be equally well explained by the single-ion factors, F_κ, in a dipole approximation of either U^{3+} or U^{4+}. The conclusions of these and the studies summarized in the following do not depend on the choice of form factor. The magnetic form factor further yields information on the ratio of the orbital to the spin moment, $R = -l/s$. The value of R is lower than the free ion value due to a partial quenching of the orbital moment. In a first study Kuwahara *et al* [15] established that the form factor under a pressure of 14 kbar increases by $(10 \pm 5)\%$.

Figure 2 shows the intensities of different Bragg peaks. The temperature dependences of the (001) and (040) peaks are identical within experimental error. As the Bragg angles of these peaks are nearly identical, this implies a high sensitivity to components perpendicular to q for either Bragg peak. The qualitative agreement of the data when going from above to below T_x implies that the moments, when entering the FM2 phase, remain aligned along the a-axes. The scaling for (001) and (111), on the other hand is not perfect below T_x. Because the Bragg angles differ for these two Bragg peaks, the relative increase of the (111) intensity by $(4 \pm 1)\%$ implies an increase of R by roughly $(15 \pm 4)\%$ when going from below to above p_x. This suggests that the ratio of the orbital to the spin moment is slightly larger above p_x,

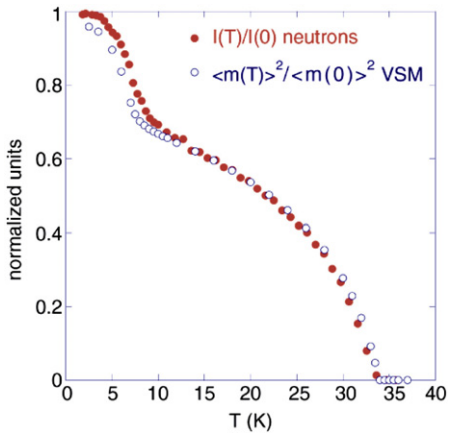

Figure 3. The normalized temperature dependence of the intensity of the (001) Bragg reflection in UGe_2 as compared to the magnetic moment squared as measured in a VSM at essentially the same pressure of 12 kbar. See [12] for further details.

consistent with the study by Kuwahara *et al* at 14 kbar [15]. If R were due to a single band, the effect of increasing pressure would be expected to delocalize the f-orbital and thus reduce R, in contrast to experiment. Thus the experiment may suggest that several interacting bands contribute to R, yielding an important clue as to the possible nature of the low-lying excitations near p_x.

A comparison of the temperature dependence of the moment squared deduced from the magnetization with the neutron data of the (001) peak is shown in figure 3. The small differences near T_x may be attributed to small differences in the applied pressure between the neutron and magnetization data. Neutron scattering data measure $\langle F_\kappa^2 M^2 \rangle$ averaged over the sample, whereas the uniform magnetization represents $\langle M \rangle$. The comparison of the (001), (010) and (040) intensities establishes that F_κ^2 changes by a few per cent between the ferromagnetic phases. Thus figure 3 displays a comparison of $\langle M \rangle^2$ with $\langle M \rangle^2$. The qualitative agreement establishes that the ferromagnetism at p_x does *not* become strongly inhomogeneous.

The same neutron scattering experiment finally also allowed us to follow the evolution of the ferromagnetic polarization as superconductivity sets in below $T_c \approx 0.7$ K. At $p = 12$ kbar the specific heat jump is the largest, and the bulk nature of the superconducting state hence the strongest. The results improve on earlier measurements down to 0.3 K performed at a pressure of 13 kbar [3]. The main observation shown in figure 4 is that there is no change of magnetic polarization through T_c to a precision of 1%. In the absence of spin–orbit coupling a strong suppression of the magnetic polarization would be expected, which is reduced in the presence of spin–orbit coupling as shown for vanadium by Shull and Wedgewood [16]. Thus at least a partial suppression of the polarization may be expected when entering the superconducting state. The observed behaviour is in contrast consistent with spin triplet pairing; an extended discussion has been given in [13].

In summary, the studies of UGe_2 establish that the miniature Cu:Be clamp cells are very well suited for diffraction experiments of small single crystals, where a direct comparison with the DC magnetization in ferromagnetic metals provides important additional information.

3. Partial order in the NFL phase of MnSi

The transition metal compound MnSi crystallizes in the cubic B20 structure (space group $P2_13$), which lacks space inversion symmetry [17]. Below $T_c = 30$ K MnSi develops

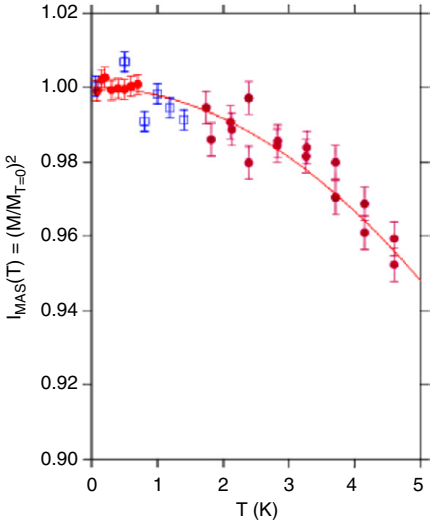

Figure 4. The temperature dependence of the intensity of the (001) Bragg reflection measured with neutrons for UGe_2 at 12 kbar. A small temperature-independent contribution due to nuclear scattering has been subtracted from the data. The remaining magnetic scattering shown is proportional to the squared magnetic polarization. There is no reduction of the polarization below $T \approx 0.7$ K at this pressure, due to superconductivity. This contrasts with observations made on conventional superconductors, where the polarization is reduced due to singlet pairing, but is consistent with triplet pairing. See [13] for a detailed discussion.

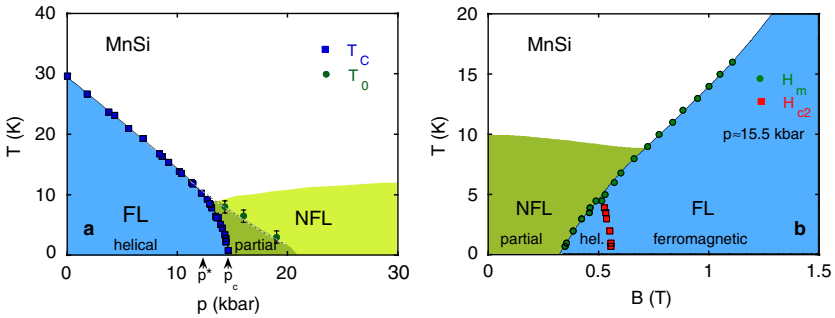

Figure 5. (a) Temperature versus pressure phase diagram of MnSi at ambient magnetic field. (b) Temperature versus magnetic field phase diagram of MnSi at $p = 15.5$ kbar. See text and [6, 8] for details.

helical spin density wave (HSDW) order with a propagation vector $Q = 2\pi/a(\zeta, \zeta, \zeta)$ with $\zeta = 0.017$ [18], that may be attributed to the Dzyaloshinsky–Moriya (DM) interaction [19, 20]. In recent years the observation that the electrical resistivity changes abruptly from a quadratic temperature dependence below $p_c = 14.6$ kbar to an exceptionally stable $T^{3/2}$ resistivity up to at least $2p_c$ has generated great interest [5–7]. This suggests the first stable non-Fermi liquid (NFL) phase in a three-dimensional metal (see figure 5).

Neutron scattering experiments were carried out [8] to search for a possible explanation of the anomalous resistivity above p_c. Studies were carried out on the cold-neutron triple-axes spectrometer 4F1 at the Laboratoire Leon Brillouin (LLB) and the small-angle spectrometer V4 at the Hahn Meitner Institut (HMI) Berlin, where neutrons were used with a wavelength of

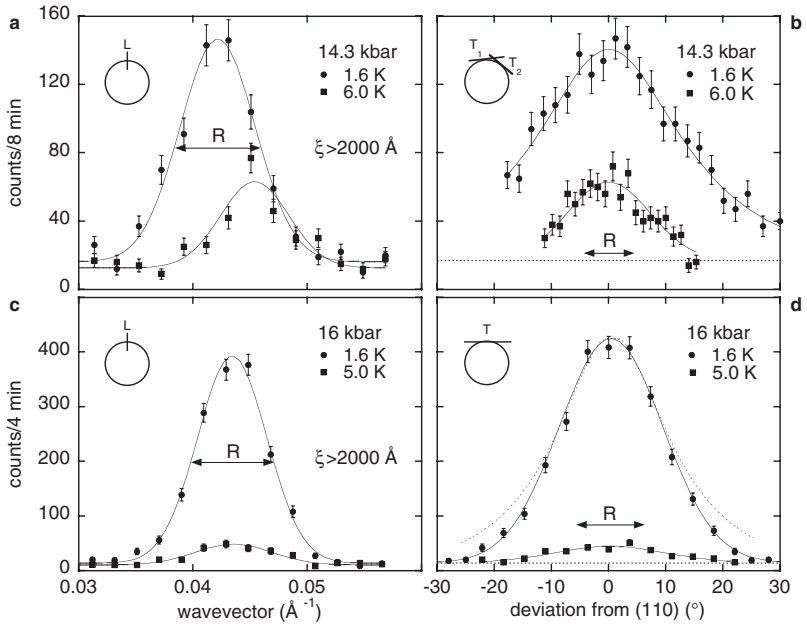

Figure 6. Typical elastic neutron scattering intensity distribution of the partial magnetic order in the non-Fermi liquid phase of MnSi, measured just above p_c. In longitudinal scans (L) through the surface of a tiny sphere in reciprocal space, resolution-limited long-range order is observed. Transverse scans (T) show in contrast that the intensity is spread over the entire sphere with a maximum at ⟨110⟩. See text and [8] for details.

1.8 and 6 Å, respectively (see [21, 22] for details of the small-angle scattering experiments). The samples studied were single crystals of dimensions $3 \times 3 \times 4$ mm^3 with a very small mosaic spread (<0.2°). Samples were pressurized in the miniature Cu:Be clamp cell described above.

Shown in figure 6 are data of the magnetic structure, observed in a pocket in the NFL phase. Instead of well defined magnetic Bragg satellites, elastic scattering intensity is found essentially everywhere on the surface of a tiny sphere with radius $Q \approx 0.043$ Å^{-1}. For longitudinal scans, resolution-limited intensity with correlation lengths $\xi > 2000$ Å is observed in agreement with long-range longitudinal order (figures 6(a) and (c)). The corresponding transverse scans shown in figures 6(b) and (d) display a very large angular spread of intensity around ⟨110⟩. In this partially ordered state the intensity peaks for different directions of the longitudinal scans at the same value of $|Q|$; that is, the intensity lies on a sphere. Hence the transverse width must not be mistaken for short-range transverse magnetic correlations, but results from a considerable variation of the directions of the spirals. This clearly establishes that the magnetic quantum phase transition (QPT) seen in the bulk properties at p_c results from an unlocking of the spiral from ⟨111⟩. It appears plausible that fluctuations related to this unlocking are the key feature of the entire NFL phase. It will be a major challenge for future inelastic neutron experiments (and complementary NMR investigations) to clarify the low-lying excitations of this state.

A special feature of the DM interactions is the prediction of a unique chirality. The selection rules in polarized neutron scattering allow us to detect this chirality [23–25]. In the small-angle scattering experiments above p_c a small magnetic field of 0.4 T was used to align the helices along a direction perpendicular to the incoming beam. Shown in figure 7 are typical intensity patterns, where the intensity surrounding the centre of the figure is the background generated by the pressure cell. The weak intensities associated with the zero-field

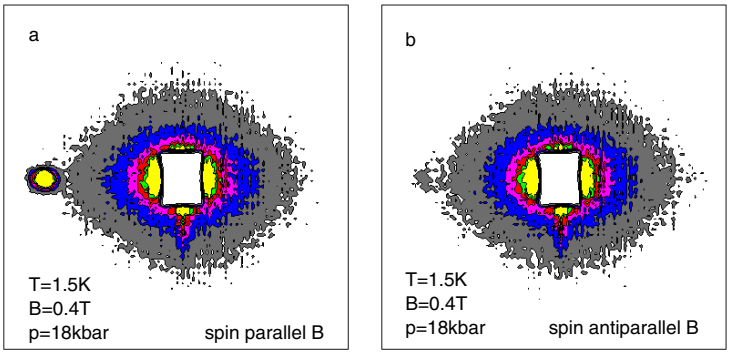

Figure 7. Typical small-angle neutron scattering pattern observed in MnSi just above p_c. The intensity around the centre is due to the pressure cell. (a) Note the spot to the left-hand side, which is due to the helical order as aligned in a magnetic field. (b) Inversion of the neutron spin with respect to the field direction leaves behind a residual intensity associated with the finite flipping ratio (≈22) of the instrument. This establishes a unique chirality of the helical order.

cooled partially ordered state are masked by this background. With increasing magnetic field, however, magnetic intensity shows up as an intense single spot shown for 0.4 T in figure 7(a). Such a narrow spot is characteristic of long-range helical order [21]. After switching off the magnetic field, the intensity of the spot is reduced, suggesting that the angular distribution of the helices widens, albeit not as much as in the zero-field cooled state. In a measurement with polarized neutrons, the magnetic Bragg peak intensity is completely suppressed on flipping the neutron spin direction relative to the magnetic propagation vector (figure 7(b)), apart from a small residual intensity associated with the finite flipping ratio (≈22) of the instrument. This observation proves that the chirality of the helical order, when aligned in a magnetic field at high pressure, is the same as that at ambient pressure.

In summary, the neutron scattering studies of MnSi at high pressure establish that the miniature Cu:Be clamp cell permits studies of long-wavelength modulated structures using cold-neutron triple-axes and small-angle neutron scattering spectrometers.

4. Quantum phase transitions in $ZrZn_2$

The search for quantum critical transitions in itinerant electron systems, which are believed to be responsible for enigmatic quantum phases like magnetically mediated superconductivity and non-Fermi liquid behaviour, has become of particular interest in recent years. However, theoretical studies suggest [26–29] that ferromagnetic transitions in clean three-dimensional (3D) itinerant ferromagnets like the C15 Laves phase compound $ZrZn_2$ at $T = 0$ are *always* first order.

Detailed measurements of the DC magnetization, i.e., direct measurements of the order parameter, have been reported in [9]. Figure 8(a) shows the ferromagnetic ordered moment M as a function of pressure and temperature (inset). The moment was obtained by extrapolating magnetization isotherms (Arrott plots) to zero field. When the pressure is varied at low temperature ($T = 2.3$ K), the magnetization drops discontinuously at the pressure $p_c = 16.5$ kbar. For comparison the inset shows the variation of the ferromagnetic moment at $p = 0$ with increasing T through the Curie temperature. At $p = 0$ the transition is continuous (second order). In contrast, when the transition is suppressed to zero through the application

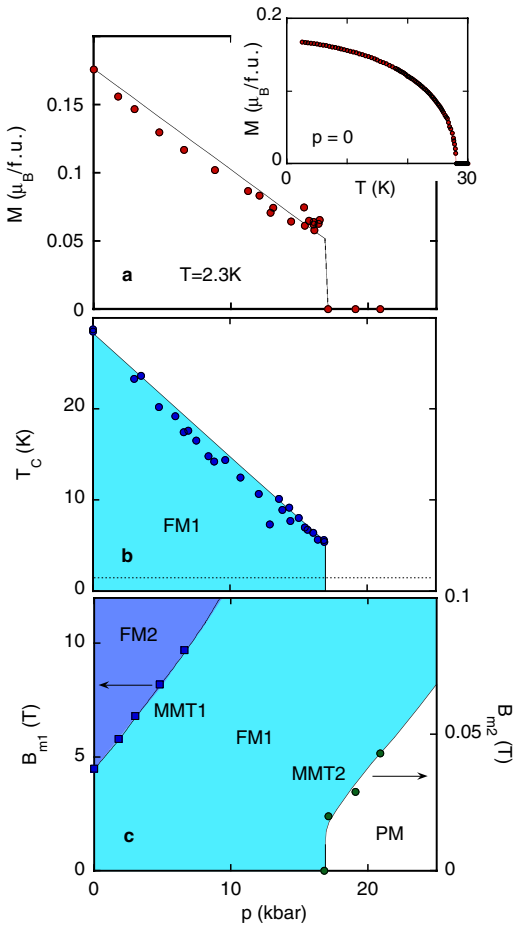

Figure 8. (a) Pressure dependence of the ordered magnetic moment M in $ZrZn_2$. See [9] for details. The ordered moment was obtained by extrapolating magnetic isotherms (Arrott plots) to zero field. The inset shows the temperature dependence of the magnetization. (b) Curie temperature T_C as a function of pressure. The dashed line marks the lowest T studied here. (c) Phase diagram determined in present measurements. MMT1 (B_{m1}) corresponds to the 'kink' or sudden change in gradient in the magnetization isotherms previously observed in [30] for $p = 0$. MMT2 (B_{m2}) corresponds a second kink observed for pressures $p > p_c$.

of hydrostatic pressure, the magnetization disappears discontinuously (first order). The Curie temperature T_C, shown in panel (b), qualitatively tracks M and vanishes also discontinuously at p_c.

Above p_c a new feature appears at low fields where $M(B)$ initially increases approximately linearly. This is followed by a sudden superlinear increase with B ('a kink'), at a field B_{m2} plotted in figure 8(c). A sudden rise in $M(B)$, such as that observed here, is usually called metamagnetism. It is the direct consequence of a local minimum of the underlying free energy and proves unambiguously that the QPT at p_c is first order. Additional measurements at high fields under hydrostatic pressure reveal a kink in the magnetization near $B \approx 5$ T. With increasing pressure B_{m1} increases as plotted in figure 8(c). The transition from FM1 to FM2 at B_{m1} corresponds to a transition *within* the ferromagnetic state, for which the moment increases by $\sim$10%. $B_{m1}(p)$ extrapolates to a QPT at approximately -6 kbar.

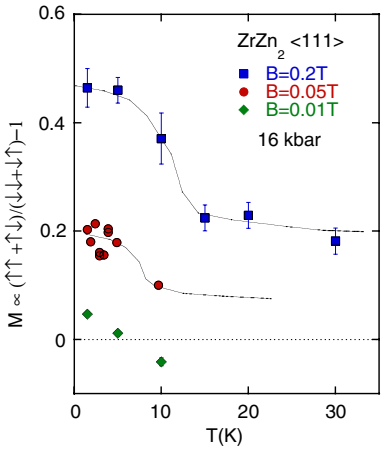

Figure 9. Ferromagnetic moment as measured at the ⟨111⟩ nuclear Bragg peak of $ZrZn_2$ at IN20 (ILL) using spin polarization analysis. A small magnetic field was applied to stabilize a single domain state. The observed temperature dependence is consistent with the high-pressure magnetization measurements [9].

The magnetization measurements establish the existence of multiple first-order QPTs in $ZrZn_2$, proposed by Kimura *et al* [31]. Various properties of the uniform magnetization in $ZrZn_2$ question, however, that the state for pressures above p_c is a simple paramagnet [32]. While the DC magnetization disappears, it is not clear if a quasi-static moment survives as in MnSi. The nature of the magnetic state at high pressure and very low fields was explored in a preliminary neutron scattering study at the thermal triple-axes spectrometer IN20 (ILL). The magnetic contribution to the ⟨111⟩ Bragg peak was measured using spin polarization analysis. Measurements were carried out in small applied fields, as indicated in figure 9. The temperature dependence was found to be consistent with the high-pressure magnetization measurements.

In summary, the studies of $ZrZn_2$ establish that high-resolution magnetization measurements permit us to measure even very small ferromagnetic signals, where the ferromagnetic signal may also be detected using a thermal neutron triple-axes spectrometer with spin polarization analysis.

5. Towards inelastic neutron scattering

The success in using the comparatively simple Cu:Be clamp cell in combination with various neutron scattering techniques motivates the question what other neutron scattering techniques may be used. For instance, the miniature clamp cells advertized here have also been used in the determination of the structure of organic compounds at the spectrometer E6 (HMI Berlin) [33]. Further, it is clear that in inelastic neutron scattering studies two technical aspects are instrumental. These are the inelastic background and the absorption of the neutrons by the pressure cell. In the course of the studies described here it was noticed that the background of the Cu:Be clamp cells in principle is extremely favourable to inelastic neutron scattering studies. In contrast, the price to be paid for the high mechanical strength of the Cu:Be is a large absorption by the Cu. In fact, preliminary experiments with a Cu:Be clamp cell in which the absorption by the cell was nearly optimized with respect to the signal by a large single crystal of MnSi suggested that inelastic studies are extremely feasible for materials with a reasonably strong signal [34].

Acknowledgments

The results shown here have been obtained in numerous collaborations as referenced throughout the text. We have also benefited from fruitful discussion with a large number of colleagues. We wish to thank in particular D Aoki, N R Bernhoeft, P Böni, A Bogdanov, E Dormann, M Enderle, B Fåk, J Flouquet, B Grenier, J Haug, B Hennion, E Garcia-Matres, B Keimer, N Kernavanois, J Kulda, B Lebech, H v Löhneysen, G G Lonzarich, J Mydosh, L Pintschovius, E Ressouche, D Reznik, B Roessli, U Rössler, A Rosch, S S Saxena, M Vojta, A Wiedenmann, P Wölfle, J Zaanen and the staff of the ILL, LLB, HMI and PSI.

References

[1] Mathur N *et al* 1998 *Nature* **394** 39
[2] Saxena S S *et al* 2000 *Nature* **406** 587
[3] Huxley A D *et al* 2001 *Phys. Rev.* B **63** 144519
[4] Pfleiderer C and Huxley A D 2002 *Phys. Rev. Lett.* **89** 147005
[5] Pfleiderer C, Julian S R and Lonzarich G G 2001 *Nature* **414** 427
[6] Pfleiderer C 2003 *Physica* B **328** 100
[7] Doiron-Leyraud N *et al* 2003 *Nature* **425** 595
[8] Pfleiderer C *et al* 2004 *Nature* **427** 227
[9] Uhlarz M, Pfleiderer C and Hayden S M 2004 *Phys. Rev. Lett.* **93** 256404
[10] Pfleiderer C 1994 *PhD Thesis* University of Cambridge
[11] Eremets M I 1996 *High Pressure Experimental Methods* (Oxford: Oxford University Press)
[12] Huxley A D *et al* 2003 *J. Phys.: Condens. Matter* **15** S1945
[13] Huxley A D *et al* 2004 *Physica* C **403** 9
[14] Kernavanois N *et al* 2001 *Phys. Rev.* B **64** 174509
[15] Kuwahara K *et al* 2002 *Physica* B **312/313** 106
[16] Shull C G and Wedgewood F A 1966 *Phys. Rev. Lett.* **16** 513
[17] Tanaka *et al* 1985 *J. Phys. Soc. Japan* **54** 2970
[18] Ishikawa Y, Tajima K, Bloch D and Roth M 1976 *Solid State Commun.* **19** 525
[19] Nakanishi O, Yanase A, Hasegawa A and Kataoka M 1980 *Solid State Commun.* **35** 995
[20] Bak P and Jensen M H 1980 *J. Phys. C: Solid State Phys.* **13** L881
[21] Pintschovius L, Reznik D, Pfleiderer C and Löhneysen H v 2004 *Pramana—J. Phys.* **63** 117
[22] Pfleiderer C, Reznik D, Pintschovius L and Löhneysen H v 2005 *Proc. SCES04*; *Physica* B at press
[23] Blume M 1963 *Phys. Rev.* **130** 1670
[24] Shirane G *et al* 1983 *Phys. Rev.* B **28** 6251
[25] Ishida M *et al* 1985 *J. Phys. Soc. Japan* **54** 2975
[26] Belitz D *et al* 1999 *Phys. Rev. Lett.* **82** 4707
[27] Vojta T 2000 *Adv. Phys.* **9** 403
[28] Belitz D and Kirkpatrick T R 2002 *Phys. Rev. Lett.* **89** 247202
[29] Shimizu M 1964 *Proc. Phys. Soc.* **84** 397
[30] Pfleiderer C *et al* 2001 *Nature* **412** 58
Pfleiderer C *et al* 2001 *Nature* **412** 660 (corrigendum)
[31] Kimura N *et al* 2004 *Phys. Rev. Lett.* **92** 197002
[32] Pfleiderer C, Uhlarz M and Hayden S M, unpublished
[33] Wosnitza J *et al* 2004 *J. Physique Coll.* IV **114** 277
[34] Pfleiderer C *et al* 2004 *PSI Report* SINQ I/04 S46